VARIABLE GEOMETRY TRACKED UNMANNED GROUNDED VEHICLE

Model, Stability and Experiments

Jean-Luc Paillat, Phillipe Lucidarme and Laurent Hardouin
Laboratoire d'Ingénierie des Systèmes Automatisés (LISA), 62 Avenue Notre Dame du Lac, Angers, France
jlpaillat@gmail.com, {philippe.lucidarme,laurent.hardouin}@istia.univ-angers.fr

Keywords: UGV (Unmanned ground vehicle), Variable Geometry Single Tracked Vehicle (VGSTV), Obstacle clearing capabilities, Teleoperation, Stability, Geometric model, Dynamic model.

Abstract: This paper introduces an originally designed tracked robot. This robot belongs to the VGSTV (Variable Geometry Single Tracked Vehicle) category. It is equipped with two tracks mounted on an actuated chassis. The first joint is used to articulate the chassis and the second one to keep the tracks tightened. By controlling the chassis joint it becomes possible to adapt the shape of the tracks to the ground and even to release the tracks in order to pass through specific obstacles. A prototype has been build ; technical specifications and dynamic model are presented in this paper. Tele-operated experiments have been conducted and have shown that the stability of the robot have to be addressed. We experimented and compared two classical criterions based on the center of mass and on the zero moment point technique. Experimental results are discussed in the case of a staircase clearing.

1 INTRODUCTION

UNMANNED GROUNDED VEHICLE (UGV) is a topically research field applied to a wide range of applications like for example exploration or missions in hostile environments. Research laboratories and robotics companies are currently working on the design of tele-operated and autonomous robots. According to (Casper and Murphy, 2003) and (Carlson and Murphy, 2005) UGVs can be classified into three categories :

- Man-packable delineates the robots that can be carried by one man in backpacks.
- Man-portable delineates the robots that are too heavy to be easily carried by men, but small enough to be transported in a car or a HUMMV.
- Not man-portable delineates the robots that must be carried by a truck, a trailer or a crane.

The robots presented in this paper are classified in the man-packable and man-portable categories. In this class of robots, designers have to face the following dilemma: on one hand, build a small robot that can be easily carried and move into narrow environments. Unfortunately, it will generally result in poor obstacle clearing capability. On the other hand, build a bigger robot will increase its ability to surmount obstacles but will not enable the robot to go through narrow openings. The challenge is then to build a robot as small as possible with the higher obstacle clearing capability. Based on this observation the first part of this paper introduces the existing experimental and commercial robots and discusses about their clearing capabilities. The following of the paper describes an originally designed UGV (Fig. 2b). This robot can be classified into the Variable Geometry Single Tracked Vehicle (VGSTV) category, i.e. it has the mechanical ability to modify its own shape according to the ground configuration. The design of our prototype is described in the third part with a short discussion about the technical choices (information can be found on the project website: http://www.istia.univ-angers.fr/LISA/B2P2/b2p2.html). The next section introduces the dynamic model of the robot. The first tele-operated experiments have shown that the mass distribution is crucial to pass through large obstacles. This is why the last section discusses about the stability of the robot. The presented survey has been conducted for three reasons. First of all, the information computed about the stability of the robot may be useful to the operator during tricky operations. Secondly, this information may also be used to automatically disable clumsy commands and prevent the robot

from toppling over. And finally, the stability cannot be ignored during autonomous motion which is our long term goal. The survey has been conducted on two criterions : static (the center of mass) and dynamic (based on the well known zero moment point technique). Experimental results are compared and discussed in the case of a staircase clearing. A general conclusion ends the paper.

2 EXISTING UGVs

2.1 Wheeled and Tracked Vehicles with Fixed Shape

This category gathers non variable geometry robots. Theoretically, this kind of vehicles are able to climb a maximum step twice less high than their wheel diameter. Therefore their dimensions are quite important to ensure a large clearing capability. This conception probably presents a high reliability (Carlson and Murphy, 2003) but those robots cannot be easily used in unstructured environments like after an earthquake (Casper and Murphy, 2003).

Figure 1: a) Talon-Hazmat robot (Manufacturer: Foster-Miller) b)ATRV-Jr robot. Photo Courtesy of AASS, Örebro University.

2.2 Variable Geometry Vehicle

A solution to ensure a large clearing capability and to reduce the dimensions consists in developing tracked vehicles which are able to modify their geometry in order to move their center of mass and climb higher obstacles than their wheel's diameters.

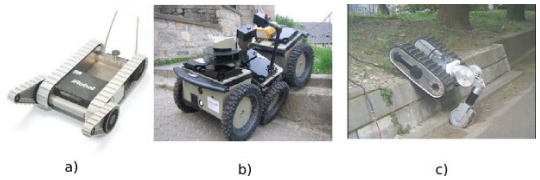

Figure 2: a)Packbot (manufacturer: IRobot), b)RobuROC 6(Manufacturer: Robosoft) c)Helios VII.

The Packbot robot (Fig. 2a) is probably one of the most famous commercial VGTV (Variable Geometry Tracked Vehicle). This robot is equipped with tracks and two actuated tracked flippers (372 mm long). The flippers are used to step over the obstacles. The obstacle clearing capability of this kind of VGTV depends on the size of the flippers. For more information and a detailed survey on clearance capability of the Packbot the reader can consult (Frost et al., 2002).

The robuROC6 (Fig. 2b) is equipped with 46.8 cm diameters wheels and can clear steps until 25cm (more than half the diameter of the wheels). Joints between the axles make this performance possible. An other original system called Helios VII (Fig 2c) (Guarnieri et al., 2004) is equipped with an arm ended by a passive wheel which is able to elevate the chassis along a curb.

2.3 Variable Geometry Single Tracked Robots

Actually, there is a subgroup in VGTV called Variable Geometry Single-Tracked Vehicles (VGSTV) (Kyun et al., 2005). It gathers robots equiped with as tracks as propulsion motors. In most cases those robots are equipped with one or two tracks (one for each side). It can be divided into two groups :

- robots with deformable tracks,
- robots with non deformable tracks.

2.3.1 Non-deformable Tracks VGSTV

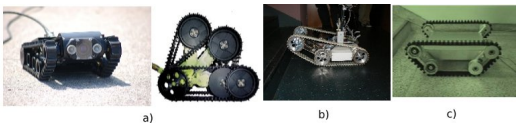

Figure 3: a) Micro VGTV (manufacturer: Inuktun Ltd) b)B2P2 prototype c)VGSTV mechanism.

The most famous example is the Micro VGTV. Illustrations of a prototypes manufactured by the company Inuktun are presented on Fig. 3a. This robot is based on an actuated chassis used to modify the shape of the robot. The right picture of Fig. 3a shows the superimposing configurations. The tracks are kept tightened by a passive mechanism. The robot is thus equipped with three motors: two for the propulsion and one for the chassis joint.

Non commercial vehicles exists in the literature as the VGSTV mechanism (Fig. 3c) which is dedicated to staircase clearing. It is composed of two tracks and two articulations which allow it to have many symmetrical configurations such as a rectangle,

trapezoids, inverse trapezoids etc.

Many other VGTV architecture exist, for further information reader can consult (Vincent and Trentini, 2007), (Misawa, 1997), (Clement and Villedieu, 1987), (Guarnieri et al., 2004) and (Kyun et al., 2005).

2.3.2 Deformable Tracks VGSTV

Some single tracked robots have the ability to modify the flexing of their tracks. Two examples presented on Fig. 4, are able to adapt their shape to obstacles (Kinugasa et al., 2008). However, even if the control of the robot seems easier with a flexible track than with a non flexible one, the mechanical conception could be more complicated.

a) b)

Figure 4: a) Viper robot (Manufacturer: Galileo) b)Rescue mobile track WORMY.

According to the presented state of the art, for general purpose missions we beleive that the best compromise between design complexity, reliability, cost and clearing capabilities is the Variable geometry single tracked robots category. The next section will introduce and describe our prototype of VGSTV.

3 PROTOTYPE DESCRIPTION

The main interest of VGSTV (equipped with deformable tracks or not) is that it is practicable to overcome unexpected obstacles (Kyun et al., 2005). Indeed, thanks to the elastic property of the tracks the clearance of a rock in rough terrain will be more smoothly with a VGSTV (e. g. Fig 3 and 4) than with a VGTV (Fig. 2). On the Micro VGTV presented on Fig. 3, the tension of the tracks is mechanically linked with the chassis joint so it is constant during the movement. Nevertheless, in some cases, less tense tracks could increase the clearance capability by increasing the adherence. An interesting study about this point was developed by (Iwamoto and Yamamoto, 1983) giving a VGSTV able to climb staircases where the tension of the tracks was mechanically managed as on the MicroVGTV (Fig. 3a). However, this system was equipped with a spring to allow the tracks to adapt their shape to the ground (depending on the strength of the spring).

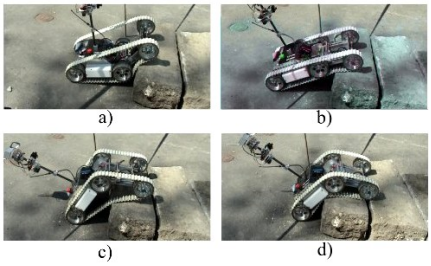

a) b) c) d)

Figure 5: B2P2: clearing of a curb.

The conception of our prototype is based on this previous work, but we decided to actuate the tension of the tracks. Indeed, by using two motors instead of one (Fig. 6) it is possible to increase the tracks adaptation to the ground developed by (Iwamoto and Yamamoto, 1983) and reach new configurations for the robot. As example, the solution proposed in this paper allows our robot to adopt classical postures of VGSTV (Fig. 5(a), 5(b) and 5(c)), but also other interesting positions. On Fig. 5 B2P2 is clearing a curb of 30 cm height with tense tracks. The position of the robot on Fig 5(c) can also be obtained with the Micro VGTV, but it is a non-safety position and B2P2 is close to topple over. On Fig. 5(d) the tracks have just been released. They take the shape of the curb and it can be cleared safely. This last configuration outlines the interest of using an active system instead of a passive one. Consequently, although our prototype (Fig. 3b) belong to the VGSTV category and have not deformable tracks, it has the ability to adapt them to the ground (as deformable ones).

Besides, even if there is a risk of the tracks coming off, loosening the tracks may be an efficient mean of increase the surface in contact with the floor in rough terrain and then to improve the clearing capability of the structure. By the way, the risk could decreased by using sensor based systems to control the tension of the tracks or by modifying the mechanical structure of the robot (adding some kind of cramps on the tracks or using a guide to get back the tracks before it comes off).

3.1 Mechanical Description

This UGV is equipped with four motors. Fig. 6 presents the integration of the motors in the robot. Motors 1 and 2 are dedicated to the propulsion (tracks).

The actuated front part is composed of motors 3 and 4 :

- Motor 3 actuates the rotational joint, it allows the rotation of the front part around the second axle.
- Motor 4 actuates a driving screw, it controls the

distance between the second axle and the third one.

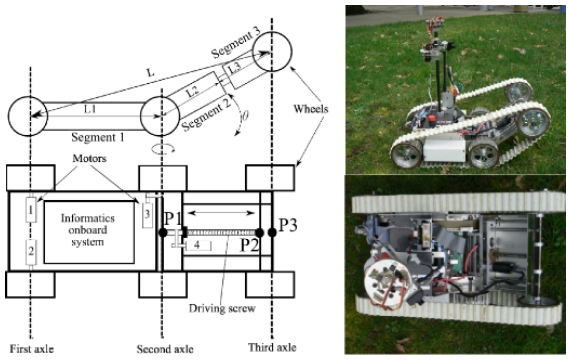

Figure 6: Overview of the mechanical structure, side and top view of the real robot.

To keep the tension of the tracks the trajectory of the third axle is given by an ellipse defined by two seats located on the first and the second axle.

$$L + (L_2 + L_3) = K \tag{1}$$

where the lengths L, L_2 and L_3 are referenced on Fig. 6. K is a constant parameter depending on the length of the tracks, L_3 evolves in order to achieve equality (1) and is linked to the angle θ in the following manner:

$$L_3 = \frac{L_1^2 - K^2}{2(L_1 cos(\pi - \mid \theta \mid) - K)} - L_2 \tag{2}$$

3.2 Sensors and Command Systems

The robot is equipped with multiple sensors, onboard/command systems and wireless communication systems.

- Onboard command systems :
  - PC104 equipped with a Linux OS compiled specifically for the robot needs based on a LFS (Home made light linux distribution).
  - An home-made I2C/PC104 interface.
  - Four integrated motor command systems running with RS232 serial ports.
  - Four polymer batteries which allow more than one hour of autonomy.
- Sensors :
  - An analog camera for tele-operation.
  - A GPS to locate the robot in outdoor environments.
  - A compass to know the orientation of the robot.
  - A two axis inclination sensor (roll and pitch).
- Wireless communication systems :
  - A 2.4 GHz analog video transmitter.
  - A bidirectional 152 MHz data transmitter.

4 DYNAMIC MODEL

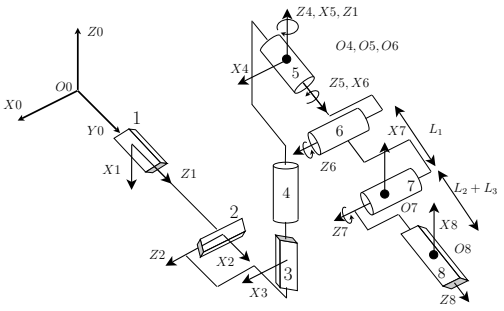

Figure 7: B2P2's geometric model. Joints 1,2 and 3 represents the robot position. Joints 4, 5 and 6 symbolize respectively the yaw, roll and pitch, 7 and 8 are the actuated joints.

This section deals with the dynamic model of the robot which is based on the geometric model (Fig. 7) detailed on (Paillat et al., 2008). According to this model, the robot motion in a 3D frame (R_0) is described by the vector q of the 8 joints variables :

$$q = [q_1, q_2, q_3, q_4, q_5, q_6, q_7, q_8]^T$$

The dynamic model of a mechanical system establishes a relation between the effort applied on the system and its coordinates, generalized speeds and accelerations ((Craig, 1989) and (Khalil and Dombre, 2004)). In this section, the following notations are used:

- j describes the joints from 1 to 8,
- i describes the segments from 1 to 3 (referenced on Fig 6),
- n and m describes indexes from 1 to 8.

4.1 The Dynamic Equations

The general dynamic equations of a mechanical system is:

$$\frac{d}{dt}\frac{\partial L}{\partial \dot{q}_j} - \frac{\partial L}{\partial q_j} = Q_j + T_j \tag{3}$$

- L is the Lagrangien of the system. It is composed of rigid segments, so there is no potential energy. Although the Lagrangien corresponds to the kinetic energy.
- q_j is the j^{th} joint variable of the system.
- Q_j is the gravity's torque applied to the j^{th} joint of the system.
- T_j is the external force's torque applied to the j^{th} joint of the system.

The kinetic energy is given by:

$$K = \sum_{i=1}^{n} \frac{1}{2} m_i v_i^T v_i + \frac{1}{2} w_i^T I_i w_i. \quad (4)$$

- m_i is the mass of the i^{th} element of the model,
- v_i is the linear speed of the i^{th} element's center of gravity,
- w_i is the angular speed of the i^{th} element's center of gravity,
- I_i is the matrix of inertia of the i^{th} element of the system.

In order to have homogeneous equations, w_i is defined in the same frame as I_i ; it allows to formulate v_i and w_i according to q :

$$v_i = J_{v_i}(q)\dot{q} \quad (5)$$

$$w_i = R_{0j}^T J_{w_i}(q)\dot{q} \quad (6)$$

where J_{v_i} and J_{w_i} are two matrices and R_{0j} is the transport matrix between the frame R_0 and the frame j linked to the segment i.

The kinetic energy formula is:

$$K = \frac{1}{2}\dot{q}^T \sum_i [m_i J_{v_i}(q)^T J_{v_i}(q) + J_{w_i}^T(q) R_{0j} I_i R_{0j}^T J_{w_i}(q)]\dot{q} \quad (7)$$

which can be rewritten as :

$$K = \frac{1}{2}\dot{q}^T D(q)\dot{q} \quad (8)$$

by developing the previous formula, we obtain :

$$K = \frac{1}{2}\sum_{m,n} d_{m,n}(q)\dot{q}_m\dot{q}_n \quad (9)$$

where $d_{m,n}(q)$ is the m,n^{th} element of the matrix $D(q)$.

The gravity's torque is given by:

$$Q_j = \sum_i g m_i \frac{\partial G_{zi}^0}{\partial q_j}. \quad (10)$$

- G_{zi}^0 is the z coordinate of the CoG of the i^{th} segment's computed in the base frame (R_0),
- g is the gravity acceleration.

Vector T (defined in (3)) is composed of the external forces' torque. For the robot presented here, there is no consideration of external forces, so the T vector only describes the motorized torques. Joints 1, 4, 7 and 8 are motorized, so the vector T is given by those four parameters. T_1 and T_4 are computed from the torques of motors 1 and 2 while T_7 and T_8 are deduced from motors 3 and 4.

The Euler-Lagrange equations can be written as:

$$\sum_m d_{jm}(q)\ddot{q}_m + \sum_{n,m} c_{nmj}(q)\dot{q}_n\dot{q}_m = Q_j + T_j \quad (11)$$

$$c_{nmj} = \frac{1}{2}[\frac{\partial d_{jm}}{\partial q_n} + \frac{\partial d_{jn}}{\partial q_m} - \frac{\partial d_{nm}}{\partial q_j}] \quad (12)$$

which is classically written as:

$$D(q)\ddot{q} + C(q,\dot{q})\dot{q} = Q + T \quad (13)$$

where $D(q)$ represents the matrix of inertia and $C(q,\dot{q})$ the centrifuge-coriolis matrix where X_{jm}, the jm^{th} element of this matrix, is defined as :

$$X_{jm} = \sum_n c_{nmj}\dot{q}_n.$$

Finally, the J_{vi} and J_{wi} matrix considered in (5) and (6) have to be computed.

4.2 J_{vi} and J_{wi} Matrix Formulation

The matrix which links articular speed and general speed of a segment is computed from the linear and angular speeds formulas. The goal is to find a matrix for each segment. They are composed of 8 vectors (one for each joint of the model).

The computation consists in formulating in the base frame, the speed ($V_{P_i}(j-1,j)^{R_0}$) of a point P_i given by a motion of the joint q_j attached to the frame j according to the frame $j-1$. Those parameters can be deduced from the law of composition speeds and the Denavitt Hartenberg (DH) formalism used for the geometric model (Paillat et al., 2008). Indeed, the general formulation is simplified by the geometric model. Only one degree of freedom (DoF) links two frames using the DH model and this DoF is a revolute or a prismatic joint. Moreover, the Z axis is always the rotation or translation axis, so the angular and linear speeds are given by four cases:

- The angular speed of a point for a revolute joint:

$$w_P(j-1,j)^{R_0} = R_{0,j} \begin{bmatrix} 0 \\ 0 \\ 1 \end{bmatrix} \dot{q_j}. \quad (14)$$

- The linear speed of a point for a revolute joint:

$$\begin{aligned} v_P(j-1,j)^{R_0} &= V_{O_j}^{R_{j-1}} + V_P^{R_j} + w_j \wedge O_j P^{R_j} \\ &= \dot{q_j} R_{0,j} \begin{bmatrix} 0 \\ 0 \\ 1 \end{bmatrix} \wedge R_{0,j} P_j. \end{aligned} \quad (15)$$

- The angular speed of a point for a prismatic joint:

$$w_P(j-1,j) = \begin{bmatrix} 0 \\ 0 \\ 0 \end{bmatrix}. \quad (16)$$

- The linear speed of a point for a prismatic joint:

$$v_P(j-1,j)^{R_0} = R_{0,j} \begin{bmatrix} 0 \\ 0 \\ 1 \end{bmatrix} \dot{q_j} \quad (17)$$

where P_j is the P point's coordinates in R_j.
Thus, the matrix of a segment i is formulated by computing speeds for each joints as :

$$\begin{bmatrix} v_i \\ w_i \end{bmatrix} = J(q)\dot{q} = [J_{1,i}(q), J_{2,i}(q), ...J_{8,i}(q)]\,\dot{q} \quad (18)$$

where $J_{j,i}(q)$ is a vector which links the speed of the i^{th} segment according to the j^{th} joint. The first segment is not affected by the motion of joints 7 and 8 while the second is not affected by joint 8, therefore $J_{7,1}(q)$, $J_{8,1}(q)$ and $J_{8,2}(q)$ are represented by a null vector.

5 BALANCE CRITERION

The balance criterion used here are the ZMP (Zero Moment Point), widely used for the stability of humanoid robots and the Center of Gravity (CoG). Previous theoretical works and experiments have proved the ZMP efficiency (Vukobratovic and Borovac, 2004). It consists in keeping the point on the ground at which the moment generated by the reaction forces has no component around x and y axis ((Kim et al., 2002) and (Kajita et al., 2003)) in the support polygon of the robot. When the ZMP is at the border of the support polygon the robot is teetering. Unlike the ground projection of the center of gravity, it takes into account the robot's inertia.

The purpose of the following is to defined the coordinates of this point in any frame of the model according to the configuration of the robot. The definition can be implemented into the Newton equations to obtain those coordinates. In any point of the model : $M_0 = M_z + OZ \wedge R$ (M_0 and M_z define respectively the moment generated by the reaction force R at the points 0 and z).

According to the previous definition, there is no moment generated by reaction forces at the Zero Moment Point. Consequently, if Z defines the ZMP coordinates $M_0 = OZ \wedge R$. This formulation can be implemented into the Newton equations as:

$$\delta_0 = M_0 + \vec{OG} \wedge \vec{P} + \vec{OG} \wedge \vec{F_i} \quad (19)$$

where P is the gravity force, G is the robot's center of gravity and F_i is the inertial force (the first Newton's law gives $F_i = -m\ddot{G}$). According to the ZMP definition, the equation (19) can be formulated as :

$$\delta_0 = \vec{OZ} \wedge \vec{R} + \vec{OG} \wedge \vec{P} + \vec{OG} \wedge \vec{F_i} \quad (20)$$

$$\begin{cases} \delta_{0x} = Z_y R_z + G_y P_z - G_z P_y - G_z F i_y \\ \delta_{0y} = -Z_x R_z + G_z P_x - G_x P_z \end{cases} \quad (21)$$

$$\begin{cases} Z_y = \frac{\delta_{0x} - G_y P_z + G_z P_y + G_z F i_y}{R_z} \\ Z_x = \frac{-\delta_{0y} + G_z P_x - G_x P_z}{R_z}. \end{cases} \quad (22)$$

Also, it is possible to compute the position of the ZMP as a function of q (δ_0 depends on the matrix $D(q)$).

Assuming the ground knowledge, the ZMP computation gives a criterion to determinate the stability of the platform.

6 RESULTS

This section presents the numerical computation of the criterion in the case of the clearance of a staircase (staircase set of 15 cm risers and 28 cm runs) with an average speed of 0.13 $m.s^{-1}$ (Fig. 9). The robot is equipped with a 2-axis inclination sensor that provides rolling and pitching. Vector q entries are measured using encoders on each actuated axis of the robot. Data have been stored during the experiments and the models (CoG and ZMP) have been computed off-line. This computation does not take into account the tracks' weight which is negligible in regard to the robot's weight. Fig. 8 presents the evolution of the ZMP (left) and the difference between those two criterion (right) during all the clearance. P_1 P_2 and P_3

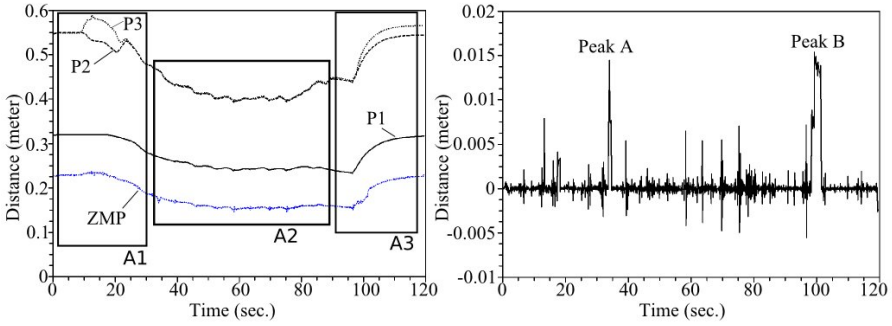

Figure 8: Experiment's results. The left chart represents the evolution of the ZMP and the right one, the difference between CoG and ZMP.

represents the z-coordinates in the frame R_5 (Fig. 7) of three points of the robot which localization are noticed on Fig. 6.

The following section finely details the results of the experiment and the correlation with the sensors data is described. This analyze is divided into three parts: the approach of the first step, the clearance of the middle steps and the clearance of the final step.

6.1 The Clearance of the First Step

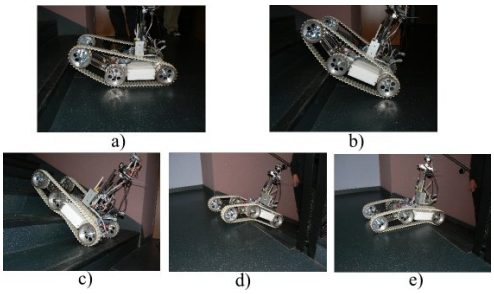

Figure 9: Clearance of a staircase.

First of all, the robot is approaching while moving up the front part (Fig. 9(a)) in order to go onto the first step. Then, it has to move forward and move down the elevation articulation in order to keep the stability (Fig. 9(b)). Once the robot is step onto the first stair, the operator have to switch in the next configuration. The area noted $A1$ on Fig. 8 shows the evolution of the ZMP projection during the clearance of the first step. Note that the tracks are tense because when the front part is rising up, there is a large difference between P_2 and P_3.

6.2 The Clearance of the Middle Steps

This stage starts in the position noticed on Fig. 9(c). By moving forward, the robot naturally climbs the stairs. At each step, the robot is gently swaying when the ZMP is passing over the step. This phenomenon is illustrated by the oscillation of the ZMP which are visible on the area noted A2 on Fig. 8. Note that, this oscillation is dependent on the ratio between the size of the robot and the size of the steps ("size-step" ratio). It fully disappears when the length of the robot is superior to the size of three steps. On the other hand, oscillations may be more important until reaching a "size-step" ratio where the robot cannot climb the step.

6.3 The Clearance of the Final Step

The robot is moving forward while moving down its front part (Fig. 9(d)). This operation brings the ZMP closer to the limits of the support polygon, i.e. the corner of the last step. This operation allows a smooth swing of the ZMP. Area A3 on Fig. 8 shows the evolution of the ZMP during the clearing of the last step.

Note that the tracks releasing was not used during this experiment because it was not necessary to overcome this staircase. It could become essential for bigger obstacles.

This experiment allows us to validate the presented model and confirms the computation of the ZMP criterion. However, as it is shown on Fig. 8, the average difference between the ZMP and the COG is insignificant (about 0.21%). Moreover, the two peaks (A and B) on the Fig. 8 are not due to the dynamics of the system but to measurement errors. As the acceleration is measured with the encoders (linked to the motor shaft), when the tracks slip, the measurement is erroneous. The ZMP is computationally more expensive, needs more sensor measurements and the difference with the CoG is negligible. For these reasons, we conclude that the CoG seems well suited for this kind of experiments. Anyway, in the case where fast obstacle clearance may be necessary, the CoG may not longer be considered and the ZMP must be used instead.

7 CONCLUSIONS

In this paper, an original prototype of VGSTV has been presented. The dynamic model have been introduced. From this model, a stability criterion based on the ZMP technique has been computed. This model have been validated on the real robot in the context of a staircase clearance.

Future works will focus on the autonomy of the robot. In a short term work, a real time stability assistance will be provided to the operator based on the model (CoG or ZMP) presented in this paper. The presented results are also a preliminary survey for a long term work that will be oriented on the autonomous obstacle clearance. Actual work (based on the model and results presented here) is focused on the automatic control of the robot.

REFERENCES

Carlson, J. and Murphy, R. R. (2003). Reliability analysis of mobile robots. *International Conferenee on Robotics and Automation*.

Carlson, J. and Murphy, R. R. (2005). How ugvs physically fail in the field. *IEEE Transactions on robotics*, 21(3):423–437.

Casper, J. and Murphy, R. R. (2003). Human-robot interactions during the robot-assisted urban search and rescue response at the world trade center. *IEEE Transactions on systems, man, and cybernetics*, 33(3):367–384.

Clement, G. and Villedieu, E. (1987). Variable geometry track vehicle. Us patent.

Craig, J. J. (1989). *Introduction to Robotics Mechanics and control*. Silma, 2 edition.

Frost, T., Norman, C., Pratt, S., and Yamauchi, B. (2002). Derived performance metrics and measurements compared to field experience for the packbot. *Proceedings of the 2002 PerMIS Workshop*.

Guarnieri, M., Debenest, P., Inoh, T., Fukushima, E., and Hirose, S. (2004). Development of helios vii : an arm-equipped tracked vehicle for search and rescue operations. *IEEE/RSJ Int. Conference on Intelligent Robots*.

Iwamoto, T. and Yamamoto, H. (1983). Variable configuration track laying vehicle (us patent).

Kajita, S., Kanehiro, F., Kaneko, K., Fujiwara, K., Harada, K., Yokoi, K., and Hirukawa, H. (2003). Biped walking pattern generation by using preview control of zero moment point. Proceedings of the 2002 IEEE Internationnal Conference on Robotics ans Automation.

Khalil, W. and Dombre, E. (2004). *Modeling, Identification and Control of Robots*. Kogan Page Science, 2 edition.

Kim, J., Chung, W. K., Youm, Y., and Lee, B. H. (2002). Real time zmp compensation method using null motion for mobile manipulators. Proceedings of the 2002 IEEE Internationnal Conference on Robotics ans Automation.

Kinugasa, T., Otani, Y., Haji, T., Yoshida, K., Osuka, K., and Amano, H. (2008). A proposal of flexible monotread mobile track. Internationnal Conference on Intelligent Robots and Systems.

Kyun, L. S., Il, P. D., Keun, K. Y., Byung-Soo, K., and Sang-Won, J. (2005). Variable geometry single-tracked mechanism for a rescue robot. *IEEE International Workshop on Safety, Security and Rescue Robotics*, pages 111–115.

Misawa, R. (1997). Stair-climbing crawler transporter. Us patent.

Paillat, J. L., Lucidarme, P., and Hardouin, L. (2008). Variable geometry tracked vehicle, description, model and behavior. Conference Mecatronics.

Vincent, I. and Trentini, M. (2007). Shape-shifting tracked robotic vehicle for complex terrain navigation: Characteristics and architecture. Technical memorandum, Defence R and D Canada.

Vukobratovic, M. and Borovac, B. (2004). Zero-momment point - thirty five years of its life. *Internationnal journal of humanoid Robotics*, 1(1):157–173.